Proceedings of ASME Turbo Expo 2011
GT2011
June 6-10, 2011, Vancouver, British Columbia, Canada

GT2011-46302

Optimization of Wind Energy Capture using BET

H. Perez-Blanco
Penn State, Mechanical Engineering
204 Reber Bldg
University Park, PA16802
hpb1@psu.edu

ABSTRACT

The Blade Element Theory (BET) has been used to predict performance of wind turbines, and to optimize energy extraction from the wind. A literature search shows that the number of parameters that can be varied to attempt optimization within BET varies for different authors. However, a repeated assumption is that the BE should be operating at the incidence angle resulting in maximum lift to drag ratio. In the present work, the incidence angle is one of the parameters varied for optimization, along with five others: the two induction factors, the chord, and the flow and setting angles. The optimization satisfies five equality constraints and three inequality constraints. The optimizer uses Levenberg-Marquardt, Conjugate Gradient or Quasi-Newton methods to maximize the power extracted. The equations adopted employ the Prandtl tip loss and require specification of the airfoil for the section, the radius of the turbine, the wind speed and the radial distribution of solidity. Up to twenty five elements can be specified for each turbine. The influence of airfoils on power coefficients is shown, and deviations from the expected maximum lift to drag positions noted. Comparisons to the performance of small wind turbines from the commercial and open literature are attempted. Whereas such comparisons are difficult in that airfoils and solidities are not often specified, they yield a baseline for establishing the validity of the optimization procedure.

INTRODUCTION

The central problem of wind energy is to interpose a surface that will capture maximum power with acceptable costs between the wind and a generator. A subset of this central problem is the optimization of wind energy capture limiting the amount of material making the surface up, while postulating different radial distributions of the material. Different approaches have been directed at this problem, often invoking the Blade Element Theory (BET), which approximates the conservation of axial and angular momentum for the BE-fluid interaction, while allowing for calculations of power harvested. One early exploration is that of Pandey (1989), where BET is used to maximize power harvested. By manipulating the BET equations under the assumption of constant lift to drag ratio to maximize power extraction, a set of non linear algebraic equations is arrived at. The system of equations is solved numerically, using the Newton-Raphson technique. Results are generated for parametric variations of the tip speed ratio and of the drag to lift ratio. The radial solidity distributions thus generated decrease with increasing radii, as also do the relative wind angles. In general, the tip speed ratios seem much more important than the drag to lift ratios in determining solidity. Increasing the tip speed ratio reduces the solidity and relative wind angles. The peak power coefficients are compatible with those found in the literature at the time, although the expectation for an optimization technique is for improvements. No specific airfoil is adopted for the research, since a constant incidence angle (i.e. the one resulting on peak lift to drag ratio) is implicitly assumed.

Morcos (1994) presents an impressive number of numerical experiments using BET, and identifies optimal operating ranges for three different blade cross sections ensuing from a parametric study. The three sections are: a flat plate, a symmetric airfoil and circular arc airfoil. The first two do not seem to offer substantial performance differences. The power coefficients are large: at solidities of 0.1 and tip speed ratios of 8, power coefficients of 0.58 are projected, and at tip speed ratios of 14, the power coefficients reach 0.59. The circular arc reaches approximately the same values. The drag to lift ratios are, once again, constant, and equal to 0.025 for the cases quoted.

A second optimization using BET is proposed by Wortman (2004). In this work, the derivative of the power coefficient with respect to wind angle is set to zero, and the equations resulting from the BET and this condition are reduced to one single function, not specified in the publication. The function is solved numerically. As in the work of Pandey (1994), a constant drag to lift ratio is specified. The power coefficients vs. tip speed are higher (for the same drag to lift ratios) than those reported by Pandey (1989). For lift to drag ratios of 0.02, the power coefficients reach 0. 55 for tip speed ratios in the range 3-5. The magnitude of the differences vary, but an upper limit of 15 % over the values of Pandey can be observed. A radial chord distribution for an optimal three blade design shows an increasing chord with radius, peaking at a dimensionless radius of 0.28, and decreasing towards the tip. Results for a NACA 0012 profile (a symmetric profile) show that the incidence angle has a strong bearing on the power coefficient. The underlying assumption is one of maximum lift to drag ratio over the whole blade.

The problem of solidity is addressed with several methods (including BET) by Duquette and Visser, 2003. Their approaches are comprehensive, including wake methods (Moriarty and Hansen 2005). When applied to an actual rotor, the wake methods and BET tend to under predict the experimental data, except at high tip speed ratios. Comparisons to commercial designs validate the approach. The BET optimal solutions of Duquette and Visser suggest high blade numbers (6-12), solidity ratios of 10 to 15%, and tip speed ratios around 4 to obtain power coefficients in the range 0.5 to 0.52.

In summary, optimization procedures for small wind turbines yield power coefficients in the range from 0.5 to 0.55 (Morco's (2004) higher values stem from an exhaustive search, not an optimization). Those values are obtained for setting angles that result in the maximum lift to drag ratio. Solidity ratios are either constant or vary with radial location. We understand the power coefficient values to exceed those attained in practice by either large or small units, but the studies are of value in that they join the mathematical logic of optimization with the practical aspects of chord and solidity distribution. The present work aims at using a larger set of variables for optimization, by letting the incidence angle and chord vary as to maximize power production. The radial solidity distribution is specified, and shown to largely influence power harvesting. The effect of different airfoils, tip speed ratio and number of blades on performance is assessed as well.

MODEL AND ASSUMED PARAMETERS

<u>Blade element theory</u>

This theory (Manwell, 2009) is a steady simplification of an essentially unsteady flow phenomenon. The wind meets the turbine at the disk plane, energy is extracted, and the velocity decreases from the original V1 to V4, Fig 1.a. The theory assumes that on the average and all along the blade, the conservation of linear and angular momentum will be heeded for the system air-blade and that the forces acting on a blade element can be calculated from lift and drag coefficients measured in wind tunnels, this is, not in a rotating blade. We present here a brief derivation of the equations used for optimization.

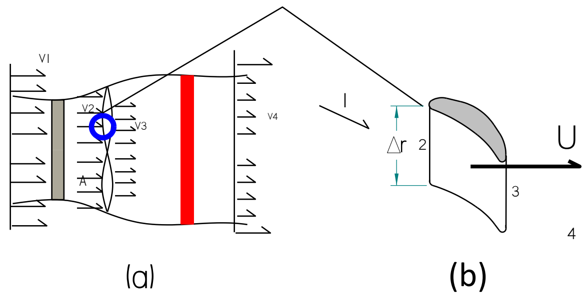

Fig 1. Wind absolute velocities and BE.

The BE is assumed to have a constant cross section, Fig .1.b, and moves with a linear velocity U. The absolute wind velocity is the vector V1. As a consequence of the flow-BE interaction, the wind velocity at the plane swept by the blades is assigned a value smaller than V1, namely:

$$V2 = (1-a)\cdot V1 \qquad \text{Eq.1}$$

The velocity V2 is also approximated as the average of upstream and downstream velocities, or

$$V2 = \frac{V1+V4}{2}$$

whereby, by virtue of Eq 1, we get

$$V4 = 2\cdot V2 - V1 = V1\cdot(1-2\cdot a) \qquad \text{Eq.2}$$

The plane that contains the rotating blades is where the flow-BE interaction takes place. The flow of momentum equals the thrust acting on the BE, namely

$$\Delta Tr = -\Delta\dot{m}\cdot(V4 - V1) \;. \qquad \text{Eq.3}$$

The mass flow rate flowing through the annulus swept by the BE is given by

$$\Delta\dot{m} = \rho\cdot V2\cdot\Delta A = \rho\cdot V2\cdot 2\cdot\pi\cdot\Delta r \qquad \text{Eq. 4}$$

Combining Eqs 2, 3 and 4, one gets

$$\Delta Tr = 4\cdot\pi\cdot\rho\cdot a\cdot(1-a)\cdot V1^2\cdot r\cdot\Delta r \qquad \text{Eq.5}$$

Before interaction with the blade, the flow direction is assumed perpendicular to the rotational plane. As angular momentum is communicated via lift forces to the BE, conservation of angular momentum requires a component of angular momentum to arise within the flow. The moment responsible for such angular momentum can then be casted for the flow affected by the BE as:

$$\Delta M = r \cdot Vu2 \cdot \Delta \dot{m}$$

which using Eq 4 becomes

$$\Delta M = \rho \cdot V2 \cdot Vu2 \cdot r \cdot \Delta A \qquad \text{Eq.6}$$

The azimuthal velocity component is approximated by

$$Vu2 = 2 \cdot ap \cdot r \cdot \Omega \qquad \text{Eq. 7}$$

Combining Eqs 6 and 7, and expressing the annulus as function of the radial interval corresponding to the BE, one has

$$\Delta M = 4 \cdot \pi \cdot \rho \cdot (1-a) \cdot ap \cdot V1 \cdot \Omega \cdot r^3 \cdot \Delta r \qquad \text{Eq.8}$$

Setting aside Eqs 5 and 8 for now, we focus now on the forces acting on a blade element, Fig 2. The lift ΔL is perpendicular, whereas the drag ΔD is parallel, to the relative wind velocity W. With the geometry of Fig 2, we have in the direction of rotation u:

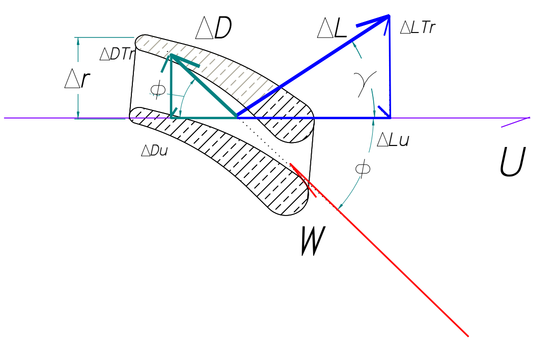

Fig 2. Blade element showing net forces.

$$\Delta Lu = \Delta L \cdot cos(\gamma) = \Delta L \cdot sin(\Phi) \qquad \text{Eq.9a}$$

$$\Delta Du = \Delta D \cdot sin(\gamma) = \Delta D \cdot cos(\Phi) \qquad \text{Eq.9b}$$

In the same fashion, the force components along the thrust direction are given by

$$\Delta LTr = \Delta L \cdot sin(\gamma) = \Delta L \cdot cos(\Phi) \qquad \text{Eq. 9c}$$

$$\Delta DTr = \Delta D \cdot cos(\gamma) = \Delta D \cdot sin(\Phi) \qquad \text{Eq. 9d.}$$

The key component of BET is now invoked: the sum of forces acting on the airfoil equals the sum of forces acting on the flow (with opposite sign). Then, we equate Eq 5 to the sum of Eqs 9a and 9b, to obtain

$$\begin{aligned}\Delta Tr &= \Delta L \cdot cos(\Phi) + \Delta D \cdot sin(\Phi) = \\ &= 4 \cdot \pi \cdot \rho \cdot a \cdot (1-a) \cdot V1^2 \cdot r \cdot \Delta r \qquad \text{Eq.10}\end{aligned}$$

Again, equating the moment of the forces as per Eq 8 and Eqs 9c and 9d, we have:

$$\begin{aligned}\Delta M &= r \cdot (\Delta L \cdot sin(\Phi) - \Delta D \cdot cos(\Phi)) = \\ &= 4 \cdot \pi \cdot \rho \cdot (1-a) \cdot ap \cdot V1 \cdot \Omega \cdot r^3 \cdot \Delta r \qquad \text{Eq.11}\end{aligned}$$

The lift and drag forces can be given as functions of the lift and drag coefficients, of the induction factors and of the relative velocity. We use Fig 3 for guidance.

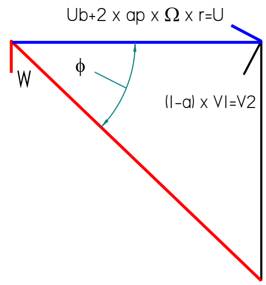

Fig 3. Velocity vectors

The magnitude of the wind-BE relative velocity is given by

$$|W| = \frac{V1 \cdot (1-a)}{sin(\Phi)}$$

And the element of lift corresponding to the BE under consideration becomes:

$$\begin{aligned}\Delta L &= \frac{1}{2} \cdot \rho \cdot W^2 \cdot Ch \cdot Cl(\alpha) \cdot \Delta r = \\ &= \frac{1}{2} \cdot \rho \cdot \frac{V1^2 \cdot (1-a)^2}{sin^2(\Phi)} \cdot Ch \cdot Cl(\alpha) \cdot \Delta r \qquad \text{Eq. 12}\end{aligned}$$

Similarly, we have for the drag force

$$\begin{aligned}\Delta D &= \frac{1}{2} \cdot \rho \cdot W^2 \cdot Ch \cdot Cd(\alpha) \cdot \Delta r = \\ &= \frac{1}{2} \cdot \rho \cdot \frac{V1^2 \cdot (1-a)^2}{sin^2(\Phi)} \cdot Ch \cdot Cd(\alpha) \cdot \Delta r \qquad \text{Eq.13}\end{aligned}$$

For thrust, we combine Eqs. 10, 12 and 13, and after some simplifications we obtain the following Eq 14:

$$1-a=\frac{8\cdot\pi\cdot r\cdot sin^2(\Phi)}{Ch\cdot(Cd(\alpha)\cdot sin(\Phi)+Cl(\alpha)\cdot cos(\Phi)}\cdot a \quad \text{Eq 14}$$

In similar fashion, we obtain from Eqs 11, 12 and 13:

$$1-a=\frac{8\cdot\pi\cdot r^2\cdot\Omega\cdot sin^2(\Phi)}{V1\cdot Ch\cdot(Cl(\alpha)\cdot sin(\Phi)-Cd(\alpha)\cdot cos(\Phi)}\cdot ap \quad \text{Eq 15.}$$

Equations 14 and 15 link the induction factors to the relative wind angle, chord and force coefficients for the airfoil. It is upon the kernel furnished by these two equations that we build the equations for optimization of energy extraction. The rate of energy extraction is directly linked to the lift and drag coefficients as follows. The power harvested by the BE is given by

$$\Delta P=U\cdot Fu$$

The force acting on the blade element along the U direction originates from the lift and it is reduced by the drag, as follows (Fig 2 and Eqs 9a and 9b)

$$\Delta P=U\cdot[\Delta L\cdot sin(\Phi)-\Delta D\cdot cos(\Phi)]$$

Using the first equalities of Eqs 12 and 13, we obtain from the above equation

$$\Delta P=\frac{\Omega\cdot r\cdot\rho\cdot V1^2}{2}\cdot\frac{(1-a)^2}{sin^2(\Phi)}\cdot Ch\cdot \cdot[Cl(\alpha)\cdot sin(\Phi)-Cd(\alpha)\cdot cos(\Phi)]\cdot\Delta r \quad \text{Eq 16}$$

Solidity ratio, relative wind angle and tip loss

Two other equations need introduction at this point. The first one concerns the solidity of the turbine. We define this in a slightly different form as customary in the literature, in order not to impose a limit on the chord while still limiting the projections on the disk. The solidity is then defined as

$$\sigma=\frac{Ch\cdot nB\cdot cos(\theta)}{2\cdot\pi\cdot r} \quad \text{Eq.17}$$

Solidity is defined as the circumferential fraction occupied by the frontal projection of the elements located at r. The second equation is commonly used by the BET, and can be understood considering Fig 3 and the tip velocity ratio, given as

$$\lambda=\frac{R\cdot\Omega}{V1} \quad \text{Eq. 18.}$$

The tangent of the relative wind angle is (Fig 3):

$$tan(\Phi)=\frac{V1\cdot(1-a)}{U}=\frac{(1-a)}{\frac{Ub+2\cdot ap\cdot\Omega\cdot r}{V1}}$$

Combining the equation above with Eq. 18, one gets, for

$$Ub=\Omega\cdot r$$

$$tan(\Phi)=\frac{(1-a)}{\lambda\cdot {}^{r}\!/_{R}\cdot(1+2\cdot ap)} \quad \text{Eq. 19}$$

There is a tip loss associated with airfoils placed on the tip of the blade. It can be shown that the tip loss extends to all the elements of the blade (Shen et al., 2005). The Prandtl tip loss (Moriarity, 2005) can be conveniently applied to the kernel Eqs 14 and 15, and has the form

$$F=\frac{2}{\pi}\cdot a\cos\left\{exp\left[\frac{-nB\cdot(R-r)}{2\cdot r\cdot sin(\Phi)}\right]\right\} \quad \text{Eq.20.}$$

OPTIMIZATION APPROACH

Since maximum power is the target, the objective function, derived from Eq 16, is

$$MAX\ (a,\Phi,Ch,\alpha)=\cdot\frac{(1-a)^2}{sin^2(\Phi)}\cdot Ch\cdot \cdot[Cl(\alpha)\cdot sin(\Phi)-Cd(\alpha)\cdot cos(\Phi)] \quad \text{Eq 21.}$$

Two other variables that do not appear in the objective function are the angular induction factor ap and the setting angle θ. For compliance with the physical model of the BE, the following constraints involving all the variables in Eq 21 plus ap and θ are invoked in the following forms

$$\Phi=a\tan\left[\frac{(1-a)}{\lambda\cdot {}^{r}\!/_{R}\cdot(1+2\cdot ap)}\right] \quad \text{Eq 19}$$

Combining Eqs 14 and 15, we obtain

$$ap=\frac{(Cl(\alpha)\cdot sin(\Phi)-Cd(\alpha)\cdot cos(\Phi)}{(Cd(\alpha)\cdot sin(\Phi)+Cl(\alpha)\cdot cos(\Phi)}\cdot\frac{V1}{r\cdot\Omega}\cdot a \quad \text{Eq 22}$$

In similar fashion, we obtain from Eqs 11, 12 and 13, and incorporating the Prandtl tip loss (Eq. 20):

$$1-a=\frac{8\cdot\pi\cdot r^{2}\cdot\Omega\cdot\sin^{2}(\Phi)}{Ch\cdot V1\cdot(Cl\cdot\sin(\Phi)-Cd\cdot\cos(\Phi))}\cdot\frac{2}{\pi}\cdot a\cos\left\{\exp\left[-\frac{nB\cdot(R-r)}{2\cdot r\cdot\sin(\Phi)}\right]\right\} \qquad \text{Eq 23}$$

The setting angle provides another constraint

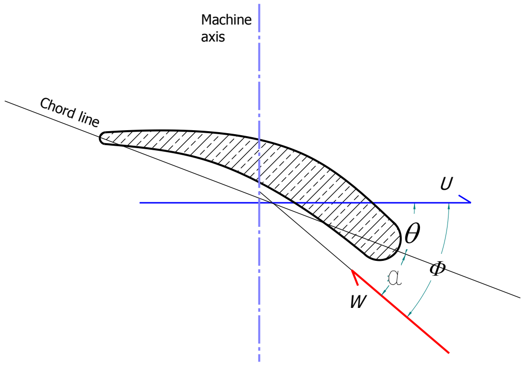

Fig 4. Setting, flow and incidence angles

$$\theta=\Phi-\alpha \qquad \text{Eq. 24}$$

Equation 17 was used in the form given above. The following obvious inequality constraints were applied

$$0\cdot\deg\le\alpha\le15\cdot\deg \qquad 0\cdot\deg\le\theta\le90\cdot\deg$$
$$0\cdot\deg\le\Phi\le90\cdot\deg \qquad \text{Eq 25.}$$

The routine used to find the maximum of Eq 21 (MathCad 14) automatically selects a method based on the rapidity of convergence to a solution. Three methods are available for non-linear problems: Levenberg-Marquardt, Quasi-Newton and Conjugate Gradient. Whereas the first two methods pursue convergence to an extreme via determination of curvature at the point under consideration in order to determine the direction to proceed, the conjugate gradient is conceptually different. Because this method is invariably chosen by the optimizer, a geometrical analog is offered here. Consider a surface in 3-D, with two independent variables, and many relative maximums and a clear “maximum maximorum”. Starting with the point defined by a set of initial guesses, the gradient (calculated numerically) points in the direction of steepest ascend. The next point in the search is taken along this direction. Actually, a number of points are considered, and the one that exhibits the steepest gradient is chosen to define the new search direction. When a maximum is identified, random amounts are added to each variable, to check whether convergence to the same extreme recurs. Convergence can occur then for a local or total maximum, or it may not occur if the surface offers flat regions.

In our case, convergence did occur after the equations were cast in the way presented by Eqs 19 to 25, including Eq 17. Starting at the hub, the guesses for each consecutive element are the converged values from the previous BE. In a few cases during the course of the work, the optimal values were changed (by introducing inequality constraints that prevented reaching the optimal solution), with the invariable result that the power harvested by the BE under consideration decreased. Hence, the optimizer seems to reach maximum values, although it is really impossible to estimate if still better values are reachable for all BEs at all conditions. The optimal set arrived at is a function of the initial guesses, and convergence in our case is often dictated by the solidity distribution adopted. The power and torque are the sum of the BE power and torque for all elements in all blades.

RESULTS

<u>Solidity ratio distributions</u>

The solidity ratio (Eq 17) and its radial distribution have a strong bearing on the optimal problem subject of this paper. The solidity ratios distributions considered in this work had the forms:

exponential: $\sigma\exp(\rho,n)=\exp(-n\cdot\rho)$ Eq. 26

power: $\sigma pow\ (\rho,n,m)=\dfrac{(1-\rho)^{n}}{m}$ Eq. 27

and constant: $\sigma c=C$ Eq 29.

The average solidity is given by

$$\bar{\sigma}=\int_{0}^{1}\sigma(\rho,n)\cdot d\rho \qquad \text{Eq 30}$$

with similar expressions for other distributions. The power coefficient is given by

$$Cp=\frac{\sum_{BE}\Delta P}{0.5\cdot\rho\cdot A_{t}\cdot V1^{3}}$$

For conditions typical for small turbines (Table 1), the solidity ratio has a strong influence on convergence and power output.

Table 1. Design conditions, typical case	
V1	10 m/s
nB	3
λ	5
Ω	191 rpm
R	2.5 m

Typically, solutions with small solidity ratios readily converge. However, small turbines tend to exhibit larger values of solidity than those with ready convergence, probably due to strength considerations. Larger solidity ratios tend to converge well for exponential distributions only, and for this reason the exponential distribution was adopted for most cases studied subsequently. Power distributions can also converge at large solidities, but the convergence is conditioned to specific initial guesses for some BEs, as opposed to simply using the optimal solution of the previous one. This makes the optimization process laborious, Selected results for different solidity ratios are shown in Table 2, where the solidity, power coefficient, average solidity and chord are presented for one airfoil, the SG6043. Data on lift and drag coefficients for all airfoils were obtained from www. aerspaceweb, 2010 and Bertagnolio et al., 2001.

Table 2. Initial experimentation with solidity

	Power (kW)	Cp	$\bar{\sigma}$	$C\bar{h}$ (cm)
$\sigma \exp(\rho,8)$	3.9	0.35	0.106	8.6
$\sigma\, pow\ (\rho,2,8)$	5.4	0.48	0.039	5.8
$\sigma\, pow\ (\rho,3,8)$	2.6	0.23	0.029	3.4
$\sigma c = 0.01$	6.4	0.57	0.01	2.7

The exponential distribution yields reliable convergence for the conditions of this study, and hence the turbine performance for different exponential solidity distributions was studied next. The results are shown in Fig 5, where the strong bearing of the solidity ratio on power coefficient is evident.

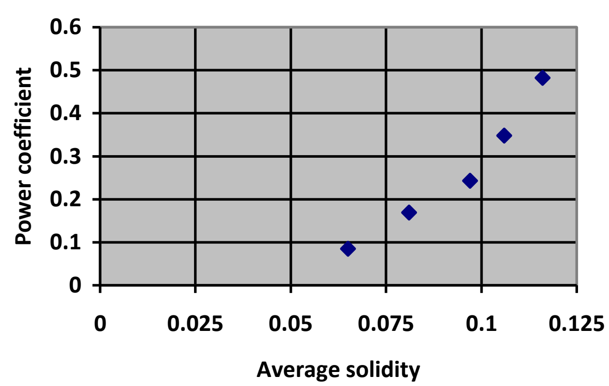

.

Fig 5. Exponential solidity and power coefficient

<u>Not all airfoils are created equal</u>

In past optimization studies, the setting angle resulting in an incidence angle value corresponding to maximum lift to drag ratio was adopted. In other words, it was assumed that the sought incidence angle could be predetermined, and that a specification of the airfoil was unnecessary. In the present work, the incidence angle and chord are independent variables with optimal values determined by the optimizer. Hence, different airfoils can yield different results, and indeed they do. For the conditions of Table 1 and exponential solidity distributions, the performance of different airfoils is recorded in Table 3. The results show that SG 6043 develops more power (3.9 kW) than the alternatives. All the airfoils result in about the same average and maximum chords, although the SG 6043 solution shows a small advantage over the others in terms of material demand.

Table 3. Performance of different airfoils at conditions of Table 1, and with $\sigma \exp(\rho,8)$

	Power (kW)	Power coeff.	Ch_{max} (cm)	$C\bar{h}$ (cm)
NACA 63-421	3.1	0.28	29	8.8
NACA 00-12	3.0	0.27	28	8.6
RISO S809	2.0	0.18	31	9
SG 6043	3.9	0.35	28	8.6

The SG6043 profile (Duquette and Visser (2003)) offers the substantial enticement of ready convergence to a better power coefficient, and it is often used in what follows. In addition to solidity ratio, the tip speed greatly influences the power coefficient, as firmly established in the literature. For the conditions of Table 1, and an exponential distribution with n equal to 8, (Eq 26), we obtain the graph in Fig 6.

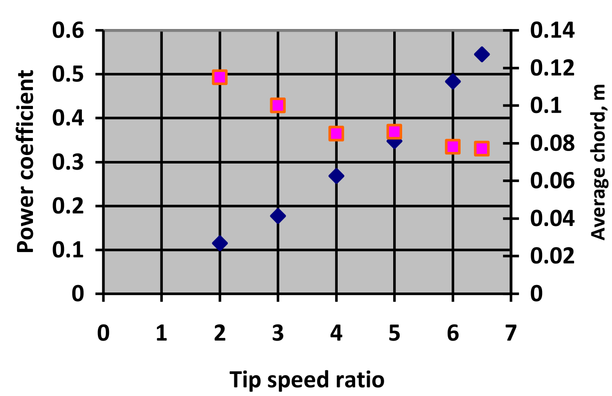

Fig 6. Exponential solidity and power coefficient

The optimal power coefficient increases with tip speed ratios, and the chord decreases. Hence, these dependences suggest an optimum in terms of material investment (which surely cannot go below the limits imposed by strength and fatigue considerations) and power output.

A few details of the distributions

Records of the power, solidity, chord and setting angle radial distributions may be of interest some readers, and they are included here to satisfy that interest. The conditions of Table 1 for the SG 6043 apply. The BE power (Fig 7) peaks at r/R of 0.3, and the chord at r/R 0f 0.1. One problem with the exponential distribution is the decrease of chord towards the tip. Whereas this fact may respond to the need of minimizing the tip loss, the values become rather small for r/R greater than 0.7. What is remarkable is that the shape of the chord distribution generally agrees with those presented in the optimal solutions of Pandey (1989) and also of Wortman (2004). The reduced chord implicit in the exponential distribution indeed decreases the BE power towards the blade tip.

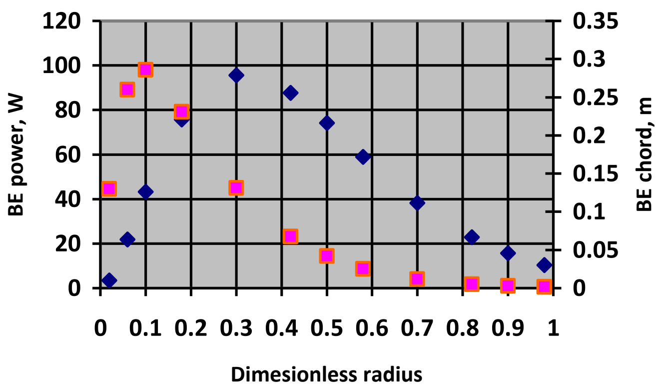

Fig7. BE power and chord distribution

The blade setting angle distribution (Fig 8) is smooth and bears resemblance to other optimal solutions (Pandey 1989), where the setting angle decreases towards the tip. The incidence angle hovers close to values that yield a lift to drag ratio of 35, whereas the airfoil under consideration exhibits a peak of 36.8 at 5.7 deg. This departure from was what assumed most desirable in previous work can be explained in terms of a multivariate optimization: the optimizer strives to find the maximum power for a set of independent variables (optimal set), yet each variable does not optimize the lift, but the rate of energy extraction.

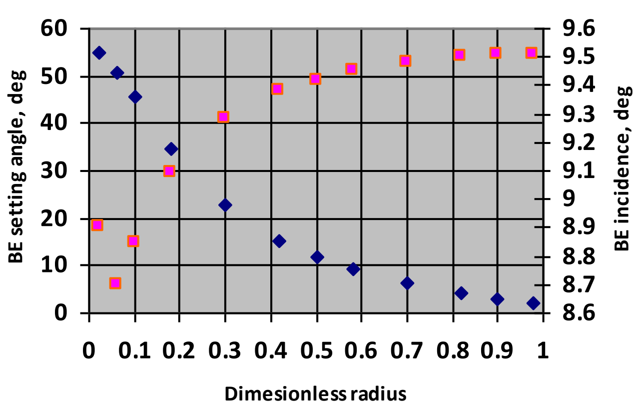

Fig 8. BE setting and incidence angle distribution

Comparison to results of related work

Once the exponential distribution was adopted, the specifications of small horizontal axis turbines were sought, to establish a performance benchmark. Whereas a working wind generator is from every possible viewpoint preferable to an optimal numerical solution, the latter may yield some insights that perhaps were not incorporated in the former. A complication ensues in that the solidity ratio of actual turbines is not part of the specs, and hence some uncertainty is always present. Of the ratings offered by Duquette and Visser (2003) , we adopted the Southwest Whisper for somewhat primitive benchmarking, Table 4.

Table 4. A small turbine and optimal solutions

	Southwest Whisper	Optimal solution, RISO	Optimal solution, NACA
R (m)	2.5	2.5	2.5
$\bar{\sigma}$	0.04	0.1	0.1
V1 (m/s)	12	12	12
nB	2	2	2
λ	10.9	11	11
$Cp \cdot \eta g$	0.154	n/a	n/a
Cp	n/a	0.33	0.574
Airfoil	n/a	RISO S809	NACA 63-421
Power, kW	3.2	1.	11.1
N, rpm	500	275	504
To, N·m	62	36	210
$\bar{Ch}$, *m*	n/a	0.055	0.105

The results of this exercise show that the optimal solution can exceed the power of the actual device, but only if the solidity is increased over the value reported (Duquette and Visser (2003)), which exhibits some uncertainty. As concluded before, optimal solutions differ with airfoils. The NACA airfoil conveys superior performance. However, there are solutions with lower solidity and tip speed ratio that are much inferior to the actual device.

Another comparison is shown in Table 5, for the Skystream 3.7 (2010) unit. Clearly, the optimal solution calls for a greater solidity ratio, since this seems like the only way to increase the power coefficient at constant wind speed and tip speed ratio. Increasing material would not only increase cost, but may also result in much slower response to wind changes.

Table 5. A small turbine and optimal solution

	Skystream 3.7	Optimal solution, NACA
R (m)	1.86	1.86
$\bar{\sigma}$	n/a	0.1
V1 (m/s)	13	13
nB	3	3
λ	5	5
$Cp \cdot \eta g$	0.06	n/a
Cp	n/a	0.28
Airfoil	n/a	NACA 63-421
Power, kW	2.4	3.8
N, rpm	333	333
To, N·m	n/a	108
$\bar{Ch}$, *m*	n/a	0.065

Yet another interesting comparison stems yet from the work of Duquette and Visser (2003). Using the BEM analysis, it is determined that for turbines such as those considered here, the optimal set will require 6 to 12 blades, a tip speed ratio of about 4, and average solidities of 10 to 15%. Solidity distributions are not specified, but it is possible to infer from other comparisons in the text that the chord is not constant, although its form of variation is unknown to this author. Using the preferred airfoil SG 6043, and the conditions of Table 1, the results illustrated in Fig 9 were produced. This plot shows the power coefficient and average chord for varying number of blades, all calculated at the optimal value of Duquesne and Visser (2003) of tip speed ratio of 4.

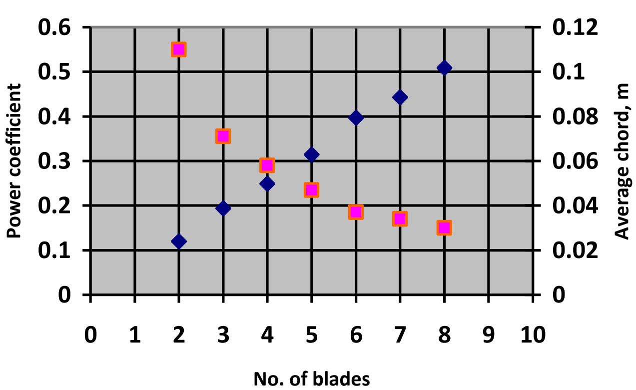

Fig 9. Power coefficient and chord for SG 6043.

Whereas the maximum solidity ratio that shows suitable convergence is 0.095, which is below the 10-15% desired, it is clear that increasing the number of blades towards the optimum arrived at by Duquette and Visser (2003) yields improved energy capture, with small chords. So, the trend of increasing blade performance for increasing number of blades is well reflected here. We note that accommodating many blades in the hub poses aerodynamic and unmet geometric challenges.

CONCLUSIONS

The computations performed with the optimizer show that the solidity ratio and its distribution have a large bearing on the power harvested. For the conditions of this study, some airfoils perform better than others, but it is unclear why. This aspect should be explored further, as should additional solidity distributions with larger solidities towards the tip of the blade. The radial setting angle and chord distributions agree in general with those of previous work, but discrepancies are evident also. For instance, the incidence angle not always coincides with the maximum lift to drag ratio, as assumed in previous optimizations. It appears that the optimizer yields solutions that could increase the power available from some small wind turbines. Yet, the dynamics and solidity distribution of such optimal solutions may be of difficult implementation. Finally, past work arrived at optimal sets that differ considerably from most small turbine designs. Investigation of the optimal set as defined by previous work shows that indeed it yields superior performance.

A persistent difficult of the BET has not been addressed, but must be noted here. The time and length scales of the wind translate into changes of the relative velocity and of the incidence angle. Whereas we project those changes to result in power loss, such projection needs to be quantified, and could be the topic of future work.

On a broader note, the present work adds to the BET, which seemed exhausted, the intriguing possibility of finding optimal solutions for new airfoils and unexplored combinations of chords and incidence angles. Whether those possibilities are indeed explored and result in valid designs remains to be seen, but the way to get there using BET would appear open.

NOMENCLATURE

a	axial induction factor.
α	wind incidence angle, deg.
ap	tangential induction factor.
A	area, m^2.
A_t	frontal turbine area, m^2.
Cd	drag coefficient.
Cl	lift coefficient.
Ch	chord, m.
γ	lift-BE velocity angle, deg.
ΔA	area increment, m^2.
ΔD	BE contribution to drag force, N.
$\Delta DTr, \Delta Du$	components of BE drag force along direction of net thrust and along rotational direction respectively, N.
ΔL	BE contribution to lift force, N.

$\Delta LTr, \Delta Lu$	components of BE lift force along direction of net thrust and along rotational direction respectively, N.
$\Delta \dot{m}$	mass flow rate increment, kg/s.
ΔM	moment of forces, N·m.
η_g	generator efficiency.
Δr	radius increment, m.
θ	BE setting angle, deg.
F	Prandtl tip loss factor.
Fu	net force on BE along rotational direction, N.
λ	tip speed ratio.
m	factor for solidity distribution, Eq 27.
n	factor for solidity distribution, Eq 26 or 27.
N	rotational velocity, rpm.
nB	number of blades.
r	radius, m.
R	turbine radius, m.
ρ	density, kg/m^3. Also, dimensionless radius r/R.
σ	solidity.
To	torque, N·m.
Tr	thrust, N
Ub	BE linear velocity along rotational direction, m/s.
U	azimuthal wind velocity component relative to BE, m/s
$V1$, $V2$, Vn	velocity at location 1,2,n, m/s
$Vu2$	azimuthal velocity component in rotational direction at point 2, m/s.
W	wind velocity relative to BE, m/s
Φ	flow angle, deg.
Ω	rotational velocity, rad/s.

ACKNOWLEDGMENTS

The author wishes to acknowledge Dr. G. Lesieutre of the Penn State Aerospace Engineering Department, for sound advice and for partial support of this work via DOE Contract No. DE-EEOOO0540, Wind Energy Workforce Development.

REFERENCES

Bertagnolio F., N. Sørensen, J. Johansen, P. Fuglsang, 2001. Wind Turbine Airfoil Catalogue. Risø-R-1280(EN). Risø Natl. Lab, Roskilde, Denmark.

Duquette M.M., K. D. Visser, 2003. "Numerical Implications of Solidity and Blade Number on Rotor Performance of Horizontal-Axis Wind Turbines." *Journal of Solar Energy Engineering* Nov. 2003, Vol. 125, pp 425-432.

MathCad 14. http://www.ptc.com/WCMS/files/95962/en /mathcad14.pdf

Manwell J.F., J. G. McGowan, A. L. Rogers 2009. Wind Energy Explained, Wiley

Morcos V. H. 1994. "Aerodynamic Performance Analysis of Horizontal Axis Wind Turbines." *Renewable Energy,* Vol. 4, No. 5, 1994, pp. 505 518,

Moriarty P.J., A.C. Hansen, 2005. AeroDyn Theory Manual. NREL/TP-500-36881. Available electronically at http://www.osti.gov/bridge

Pandey M. M., K.P. Pandey, T.P. Ojha, 1989. "An Analytical Approach to Optimum Design and Peak Performance Prediction for Horizontal Axis Wind Turbines." *Journal of Wind Engineering and Industrial Aerodynamics,* 32 (1989) 247-262.

Shen W. Z., R. Mikkelsen, J. N. Sørensen, 2005. "Tip Loss Corrections for Wind Turbine Computations." *Wind Enery.* 2005; **8**:457–475. Published online 31 March 2005 in Wiley Interscience (www.interscience.wiley.com). DOI: 10.1002/we.153

Skystream 3.7 http://www.windenergy.com/documents/brochures/ 3-CMLT-1344-01_Skystream_brochure.pdf

Wortman A., 2004. "Optimum Performance and Design Procedures for Propeller Wind Turbines with Non-ideal Airfoil Sections." *42nd AIAA Aerospace Sciences Meeting and Exhibit 5 - 8 January 2004, Reno, Nevada*. AIAA-2004-1363.

www. aerospaceweb.org/question/airfoils.